JOURNAL OF Materials CHEMISTRY

New mixed valent vanadium monophosphate with an intersecting tunnel structure $Ba_2V_5O_8(PO_4)_4$

M. M. Borel, A. Leclaire,*† J. Chardon and B. Raveau

Laboratoire CRISMAT, UMR 6508 CNRS, ISMRA, Bd du Maréchal Juin 14050, Caen cedex, France

A new mixed valent vanadium monophosphate $Ba_2V_5O_8(PO_4)_4$ has been synthesized. It crystallizes in the space group $I1m1$ with $a=7.6405(1)$, $b=22.777(1)$, $c=11.6157(7)$ Å and $\beta=103.38(1)°$. Its framework consists of $[V_4P_4O_{22}]_\infty$ layers of corner sharing polyhedra, interconnected by VO_4 tetrahedra which delimit tunnels in which the barium atoms are located. The vanadium atoms exhibit three kinds of coordination; pyramidal, octahedral and tetrahedral, in the same framework.

Transition metal phosphates offer a wide field of investigation owing to their great ability to form numerous original structures. Mixed valency of the transition element is of great interest for the generation of particular magnetic and transport properties, and also of catalytic properties for oxidation of organic molecules.

This is especially the case of vanadium phosphates which exhibit a large number of original structures owing to the fact that vanadium adopts various coordinations (tetrahedral, octahedral, pyramidal) and various oxidation states ranging from V^{II} to V^{V}. For instance the VPO system and in particular $(VO)_2P_2O_7$ have been shown to be excellent catalysts in the conversion of butane to maleic anhydride (see for instance refs. 1–5). The recent study of the phosphates $A(VO)_2(PO_4)_2$ (A = Cd, Ca, Pb, Ba)[6–10] suggests that the phosphates of divalent elements may be of interest as catalysts for propene oxidation although the influence of the structure and the oxidation state of vanadium on those properties is so far not clear. For this reason a systematic exploration of vanadium phosphates containing divalent cations should be performed. On this basis we have reinvestigated the Ba–V–P–O system, for which very few compounds have been synthetized to date, compared to vanadophosphates of univalent elements. Only five vanadophosphates containing barium have indeed been isolated: three of them, α- and β-$BaV_2(P_2O_7)_2$[11,12] and $Ba_3V_4(PO_4)_6$ [13] contain trivalent vanadium, whereas in the two others, $Ba(VO)_2(PO_4)_2$ [9] and $BaVO_2PO_4$,[14] vanadium is tetravalent and pentavalent, respectively. In the present work we report on the first barium vanadophosphate that exhibits a mixed valence of vanadium, $Ba_2V_5O_8(PO_4)_4$. The original structure of this phase that displays three types of coordination for vanadium, tetrahedral, pyramidal and octahedral, is described.

Experimental

Synthesis

Based on our previous investigations of the Ba–V–P–O system, attempts were made to synthesize new mixed valent vanadophosphates. Various compositions corresponding to different $V^V:V^{IV}$ ratios were studied. A new phase was identified for $V^V:V^{IV}\approx4:1$ and for $P:V:Ba\approx2:2:1$. The EDS analysis of this new phase revealed its exact cationic composition '$Ba_2V_5P_4$', then a systematic exploration of the nominal compositions '$Ba_2V_5P_4O_x$' was carried out for x ranging from 22 to 24.5. The powder X-ray diffraction investigation of the different products evidenced a pure phase for the composition $Ba_2V_5P_4O_{24}$; this composition was then confirmed later by the single crystal structure determination.

The synthesis of the vanadophosphate $Ba_2V_5O_8(PO_4)_4$ was perfomed in two steps. First an intimate mixture of $Ba(NO_3)_2$, NH_4VO_3 and $H(NH_4)_2PO_4$ in adequate ratios according to the composition $Ba_2V_{4.8}P_4O_{24}$ was heated at 673 K for 4 h in a platinum crucible to decompose the barium nitrate, ammonium vanadate and ammonium phosphate. In a second step, the resulting mixture was then added to the required amount of vanadium (0.2 mol) sealed in an evacuated silica ampoule then heated for 12 h at 823 K, and finally quenched at room temperature.

The product was a dark green powder. The powder X-ray diffraction pattern of the latter was indexed in a monoclinic cell in agreement with the parameters obtained from the single crystal X-ray study.

Crystal growth

In order to obtain single crystals of the new phase, we have incorporated a lithium salt in several compositions since recently the presence of lithium allowed us to grow single crystals of a new phosphate $Ba_3Mo_2O_2(PO_4)_4$.[15] Indeed single crystals were extracted from a mixture of nominal composition $LiBaV_2P_4O_{16}$ synthesized from Li_2CO_3, $BaCO_3$, VO_2 and $H(NH_4)_2PO_4$ in the molar ratios 1:1:2:4 . The mixture was heated in air in a platinum crucible first at 673 K for 3 h then after grinding, it was heated in air at 823 K for 2 days, cooled at 5 K h^{-1} to 673 K and finally quenched to room temperature.

In the resulting mixture two sorts of crystals have been extracted : blue plates, always twinned not yet identified and a few black crystals. The microprobe analysis of these black crystals leads to V/P/Ba ratios in agreement with the formula $Ba_2V_5P_4O_{24}$ deduced from the structure determination.

Energy dispersive analysis (EDS)

Elemental analysis of Ba, V, P was performed with a Tracor microprobe mounted on a scanning electron microscope. The atomic ratios obtained (18% Ba, 45% V and 57% P) established the '$Ba_2V_5P_4$' composition in agreement with the structure determination.

X-Ray diffraction study

Different crystals were tested by Weissenberg method using Cu-Kα radiation.

A black crystal with dimensions $0.077\times0.051\times0.051$ mm was selected for the structure determination. The cell parameters were determined by diffractometric techniques at 294 K with a least squares refinement based upon 25 reflections with

† E-mail: leclaire@crcrisu.ismra.fr

$18 < \theta < 22°$. The data were collected on a CAD4 ENRAF NONIUS diffractometer with parameters reported in Table 1. The reflections were corrected for Lorentz and polarisation effects and for absorption.

The systematic extinction $h+k+l=2n+1$ for *hkl* is consistent with the space groups $I12/m1$ and $I1m1$ The refinement of the structure was successful in the non-centrosymmetric group *Im*. The structure was solved using the heavy atom method.

The refinement of the atomic coordinates, of isotropic thermal factors for the oxygen atoms and anisotropic thermal factors for the other atoms led to $R=0.034$ and $R_w=0.035$. The calulations were performed on a SPARK station with the XTAL3.2 programs.[16]

Full crystallographic details, excluding structure factors, have been deposited at the Cambridge Crystallographic Data Centre (CCDC). See Information for Authors, *J. Mater. Chem.*, 1998, Issue 1. Any request to the CCDC for this material should quote the full literature citation and the reference number 1145/77.

Table 1 Summary of crystal data, intensity measurements and structure refinement parameters for $Ba_2V_5P_4O_{24}$

crystal data	
space group	$I1m1$
cell dimensions	$a=7.6705(5)$ Å
	$b=22.777(1)$ Å $\beta=103.38(1)°$
	$c=11.6157(7)$ Å
volume/Å^3	1974.3(2)
Z	4
D_c/g cm^{-3}	3.49
intensity measurements	
λ(Mo-Kα)/Å	0.71073
scan mode	ω–$4/3\theta$
scan width/degrees	$1+0.35\tan\theta$
slit aperture/mm	$1+\tan\theta$
max. θ/degrees	45
standard reflections	3 every 3600 s
measured reflections	8514
reflections with $I>3\sigma(I)$	2608
μ/mm^{-1}	6.53
structure solution and refinement	
parameters refined	205
agreement factors	$R=0.034$ $R_w=0.030$
weighting scheme	$w=1/\sigma^2$
Δ/σ max.	<0.001
$\Delta\rho$/e Å^{-3}	1.9 near Ba(1)

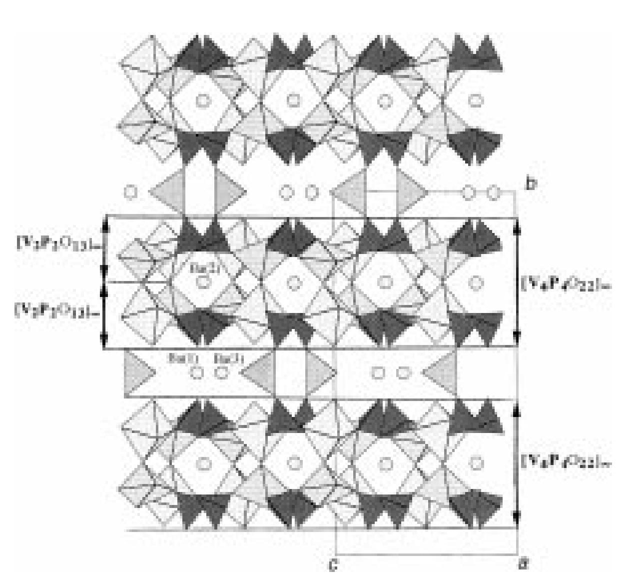

Fig. 1 Projection of the structure of $Ba_2V_5O_8(PO_4)_4$ along ***a***

Results and Discussion

Structure

The atomic coordinates of this new structure are listed in Table 2. The projection of this framework along ***a*** (Fig. 1) shows the following features.

(*i*) The vanadium atom exhibits three types of coordination: pyramidal [V(1), V(2)], octahedral [V(3), V(4)] and tetrahedral [V(5), V(6)]. The existence of these three coordination modes for vanadium in the same structure is rare: it has never been observed, to our knowledge, for vanadium phosphates.

(*ii*) The VO_5 pyramids and VO_6 octahedra share their corners forming V_4O_{18} units in which each V(1) [or V(2)] pyramid is linked to two VO_6 octahedra [V(3) and V(4)].

(*iii*) The V_4O_{18} are linked through monophosphate groups, forming $[V_2P_2O_{13}]_\infty$ layers parallel to (010).

(*iv*) Two successive $[V_4P_4O_{22}]_\infty$ layers are interconnected along ***b*** through VO_4 tetrahedra [V(5), V(6)]. The latter share two of their apices with two PO_4 tetrahedra of two different layers [P(1), P(4)], so that they form tetrahedral P_2VO_{10} strings rings running along ***b***.

(*v*) This framework of corner sharing polyhedra delimits two sorts of tunnels running along ***a***: large butterfly shaped tunnels located at the level of the VO_4 tetrahedra where the Ba(1) and Ba(3) cations are located, and six-sided tunnels located within the $[V_4P_4O_{22}]_\infty$ layers, occupied by Ba(2).

(*vi*) Each VO_4 tetrahedron [V(5) or V(6)] has two free apices, whereas each PO_4 tetrahedron [P(1), P(2), P(3), P(4)] has one free apex. Note that all the free apices of these polyhedra are directed toward the axis of the 'butterfly-like tunnels'.

(*vii*) The $[V_4P_4O_{22}]_\infty$ layer consists of two enantiomorphic $[V_2P_2O_{13}]_\infty$ layers turned by 180° with respect to each other and connected in such a way that one VO_5 pyramid of one layer be linked to one VO_6 octahedron of the other.

The projection of one $[V_2P_2O_{13}]_\infty$ layer along ***b*** (Fig. 2) shows that it is built up from $[V_2P_2O_{15}]_\infty$ chains running along [101] in which the VO_5 pyramids, the VO_6 octahedra and the PO_4 tetrahedra alternate according to the sequences P(2)V(2)P(1)V(4)P(2) and P(3)V(3)P(4)V(1)P(3), labelled C1 and C2 respectively. The latter are assembled along [101] according to the sequence C1–C2–C1. Each C1 (or C2) chain shares on one side the apices of its VO_5 and of its VO_6 octahedra with those of the VO_6 octahedra and of the VO_5 pyramid of the next C2 (or C1) chain respectively. These chains form six-sided windows built up of two VO_5 pyramids, two VO_6 octahedra and two PO_4 tetrahedra similar to those observed in the brownmillerite, and diamond shaped windows built up of two PO_4 tetrahedra and two VO_5 pyramids or two VO_6 octahedra.

The $[V_5P_4O_{24}]_\infty$ framework also delimits six- and four-sided tunnels running along ***b***, as shown from the projection

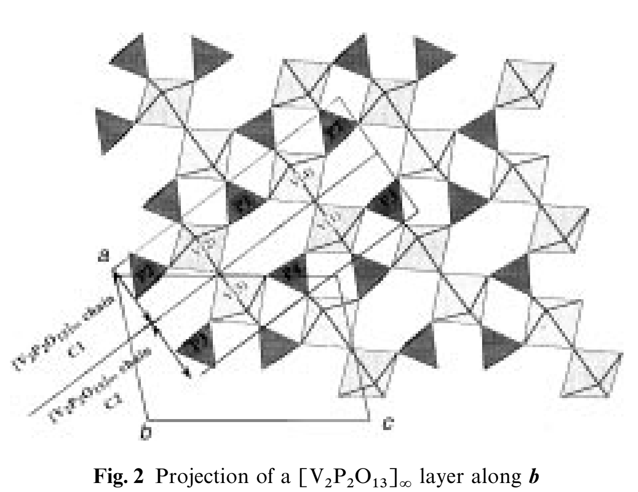

Fig. 2 Projection of a $[V_2P_2O_{13}]_\infty$ layer along ***b***

Table 2 Atomic positional, isotropic and anisotropic displacement parameters

atom	x/a	y/b	z/c	$U/\text{Å}^2$	atom	x/a	y/b	z/c	$U/\text{Å}^2$
Ba(1)	0.26000	0.0000	0.26000	0.0150(3)*	O(8)	0.053(1)	0.1792(3)	0.2556(7)	0.012(2)
Ba(2)	0.2525(2)	0.24897(3)	0.7205(1)	0.0137(2)*	O(9)	0.355(1)	0.1263(4)	0.3604(7)	0.010(2)
Ba(3)	0.6990(2)	0.0000	0.1218(1)	0.0118(3)*	O(10)	0.347(1)	0.1684(4)	0.5670(8)	0.020(2)
V(1)	0.3076(3)	0.18674(8)	0.0408(2)	0.0072(5)*	O(11)	0.896(1)	0.0733(4)	0.5017(7)	0.018(2)
V(2)	0.2040(3)	0.18186(9)	0.4091(2)	0.0073(5)*	O(12)	0.659(1)	0.1267(4)	0.5990(7)	0.016(2)
V(3)	0.8489(3)	0.13802(9)	0.5268(2)	0.0084(5)*	O(13)	0.002(1)	0.1503(3)	0.6851(7)	0.011(1)
V(4)	0.6603(3)	0.14294(9)	0.9253(2)	0.0082(5)*	O(14)	0.681(1)	0.1570(3)	0.3805(7)	0.010(2)
V(5)	0.1265(4)	0.0000	0.9155(3)	0.0124(8)*	O(15)	0.587(1)	0.0790(4)	0.9449(7)	0.022(2)
V(6)	0.3896(4)	0.0000	0.5711(3)	0.0147(9)*	O(16)	0.857(1)	0.1269(4)	0.8525(7)	0.013(2)
P(1)	0.4916(4)	0.1309(2)	0.6479(3)	0.0081(9)*	O(17)	0.520(1)	0.1624(3)	0.7678(7)	0.009(1)
P(2)	0.0030(4)	0.1320(1)	0.1558(3)	0.0067(8)*	O(18)	0.831(1)	0.1577(3)	0.0771(6)	0.009(2)
P(3)	0.5132(4)	0.1308(2)	0.2966(3)	0.0088(9)*	O(19)	0.299(2)	0.0000	0.023(1)	0.025(3)
P(4)	0.0290(4)	0.1287(2)	0.8129(3)	0.0077(8)*	O(20)	−0.040(2)	0.0000	0.977(1)	0.024(3)
O(1)	0.247(1)	0.2523(4)	0.0604(7)	0.015(2)	O(21)	0.114(1)	0.0674(4)	0.8239(7)	0.017(2)
O(2)	0.495(1)	0.1933(3)	0.0149(7)	0.010(1)	O(22)	0.524(2)	0.0000	0.484(1)	0.022(3)
O(3)	0.157(1)	0.1290(3)	0.0901(7)	0.011(2)	O(23)	0.188(2)	0.0000	0.481(1)	0.028(3)
O(4)	0.162(1)	0.1737(4)	−0.1189(7)	0.016(2)	O(24)	0.420(1)	0.0682(4)	0.6588(7)	0.023(2)
O(5)	0.467(1)	0.1780(3)	0.199(1)	0.018(2)	O(25)	−0.023(1)	0.0726(3)	0.2063(8)	0.015(2)
O(6)	0.265(1)	0.2481(4)	0.4046(7)	0.020(2)	O(26)	0.542(1)	0.0711(4)	0.2497(8)	0.016(2)
O(7)	0.017(1)	0.1820(3)	0.4720(7)	0.012(1)					

	U_{11}	U_{22}	U_{33}	U_{12}	U_{13}	U_{23}
Ba(1)	0.0102(4)	0.0121(4)	0.0242(5)	0	0.0070(4)	0
Ba(2)	0.0125(2)	0.0098(2)	0.0207(3)	0.0010(3)	0.0078(2)	0.0021(3)
Ba(3)	0.0104(4)	0.0105(4)	0.0159(5)	0	0.0058(4)	0
V(1)	0.0062(8)	0.0088(8)	0.0058(9)	−0.0002(7)	0.0001(6)	−0.0003(7)
V(2)	0.0051(8)	0.0121(9)	0.0045(8)	0.0003(7)	0.0007(6)	−0.0003(7)
V(3)	0.0070(9)	0.0119(9)	0.0054(9)	0.0006(7)	−0.0003(7)	0.0008(7)
V(4)	0.0051(9)	0.0137(9)	0.0051(8)	−0.0006(7)	−0.0002(7)	0.0019(7)
V(5)	0.016(1)	0.010(1)	0.012(1)	0	0.004(1)	0
V(6)	0.015(1)	0.011(1)	0.019(1)	0	0.005(1)	0
P(1)	0.008(1)	0.011(2)	0.006(1)	0.001(1)	0.001(1)	−0.002(1)
P(2)	0.006(1)	0.009(1)	0.004(1)	−0.001(1)	0.001(1)	−0.000(1)
P(3)	0.007(1)	0.010(2)	0.009(1)	−0.003(1)	0.002(1)	−0.002(1)
P(4)	0.004(1)	0.011(2)	0.007(1)	−0.001(1)	0.000(1)	−0.001(1)

* U_{eq} deduced from anisotropic U_{ij}.

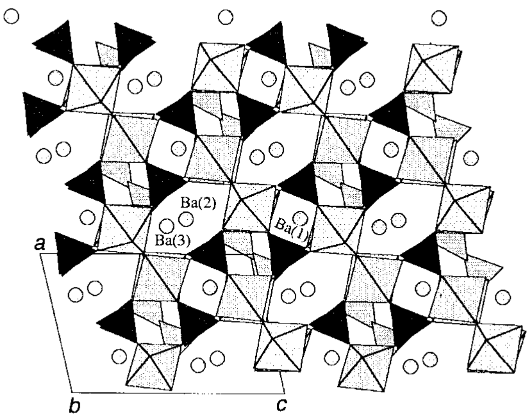

Fig. 3 Projection of the structure of $Ba_2V_5O_8(PO_4)_4$ along ***b***

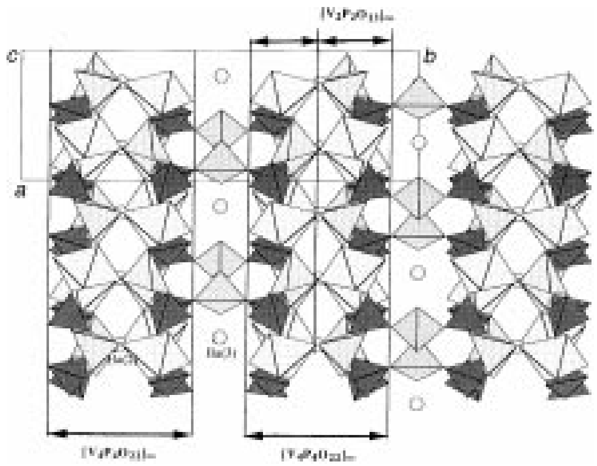

Fig. 4 Projection of the structure of $Ba_2V_5O_8(PO_4)_4$ along ***c***

of the structure along ***b*** (Fig. 3). The first type of tunnel is occupied by Ba(2) and Ba(3), whereas Ba(1) sits in the second type. In the same way, the projection of the structure along ***c*** (Fig. 4) shows the existence of large tunnels running along this direction and occupied by Ba(3). Clearly the monophosphate $Ba_2V_5O_8(PO_4)_4$ can be described as an intersecting tunnel structure, the barium cations sitting at the intersection of these tunnels.

Another way to describe this framework is to consider the (110) layers that are one polyhedron thick (Fig. 5). In these layers two $[V_2P_2O_{13}]_\infty$ chains running along [101] form [110] ribbons by sharing the apices of their VO_5 pyramids and VO_6 octahedra, and two successive ribbons are interconnected through VO_4 tetrahedra; one recognizes that each VO_4 tetrahedron is linked to two PO_4 tetrahedra, forming the VP_2O_{10} units. In these layers one observes six-sided brownmillerite type windows, and much larger windows limited by twelve polyhedra. Such windows correspond to the six-sided and butterfly like tunnels respectively, running along ***a*** (Fig. 1). The entire $[V_5P_4O_{24}]_\infty$ framework results then from the stacking of identical $[V_2P_2O_{13}]_\infty$ layers along $[10\bar{1}]$, two successive layers sharing the apices of their polyhedra, according to the description made above for the connection of the $[V_2P_2O_{15}]_\infty$ chains.

The distances and angles in the polyhedra of this structure are listed in Table 3.

The P(1) and P(4) tetrahedra share their four apices with two VO_6 octahedra, one VO_5 pyramid and one VO_4 tetra-

Table 3 Distances (Å) and angles (°) in the polyhedra for $Ba_2V_5P_4O_{24}$

V(1)	O(1)	O(2)	O(3)	O(4)	O(5)
O(1)	**1.594(9)**	2.64(1)	2.93(1)	2.71(1)	2.65(1)
O(2)	105.6(5)	**1.717(9)**	3.44(1)	2.61(1)	2.56(1)
O(3)	112.6(5)	141.8(4)	**1.925(9)**	2.64(1)	2.67(1)
O(4)	99.0(4)	90.1(4)	85.8(4)	**1.955(8)**	3.89(1)
O(5)	95.7(4)	88.0(4)	86.6(4)	165.1(4)	**1.97(1)**

V(2)	O(6)	O(7)	O(8)	O(9)	O(10)
O(6)	**1.585(9)**	2.69(1)	2.61(1)	2.93(1)	2.59(1)
O(7)	106.8(5)	**1.757(9)**	2.59(1)	3.41(1)	2.54(1)
O(8)	96.9(4)	90.7(4)	**1.890(8)**	2.65(1)	3.80(1)
O(9)	114.9(5)	138.1(4)	88.9(4)	**1.890(9)**	2.60(1)
O(10)	94.4(4)	86.9(4)	168.7(4)	85.6(4)	**1.933(9)**

V(3)	O(11)	O(12)	O(14)	O(7^{i})	O(13^{i})	O(1^{ii})
O(11)	**1.561(9)**	2.65(1)	2.69(1)	2.69(1)	2.73(1)	4.23(1)
O(12)	101.1(4)	**1.86(1)**	2.67(1)	3.63(1)	2.65(1)	2.90(1)
O(14)	100.5(4)	89.7(4)	**1.929(8)**	2.61(1)	3.82(1)	2.90(1)
O(7^{i})	103.8(4)	155.1(4)	87.2(4)	**1.855(9)**	2.60(1)	2.92(1)
O(13^{i})	101.3(4)	87.7(4)	158.2(4)	86.1(4)	**1.960(8)**	3.09(1)
O(1^{ii})	176.3(4)	77.2(4)	76.2(4)	78.1(4)	82.1(4)	**2.672(9)**

V(4)	O(15)	O(16)	O(17)	O(2^{iii})	O(18^{iii})	O(6^{ii})
O(15)	**1.597(9)**	2.77(1)	2.76(1)	2.76(1)	2.78(1)	4.23(1)
O(16)	103.2(4)	**1.930(9)**	2.67(1)	3.79(1)	2.75(1)	3.03(1)
O(17)	101.9(4)	87.1(4)	**1.946(7)**	2.67(1)	3.83(1)	2.97(1)
O(2^{iii})	101.9(4)	154.9(4)	86.5(4)	**1.950(7)**	2.68(1)	2.80(1)
O(18^{iii})	102.2(4)	89.9(4)	155.8(3)	86.2(4)	**1.968(7)**	2.90(1)
O(6^{ii})	175.2(4)	81.5(4)	79.2(3)	73.5(3)	76.5(3)	**2.636(9)**

V(5)	O(19^{iii})	O(20)	O(21)	O(21^{iv})
O(19^{iii})	**1.59(1)**	2.53(1)	2.86(1)	2.86(1)
O(20)	104.7(4)	**1.60(2)**	2.81(1)	2.81(1)
O(21)	111.9(4)	108.3(4)	**1.86(1)**	3.07(1)
O(21^{iv})	111.9(4)	108.3(4)	111.5(4)	**1.86(1)**

V(6)	O(22)	O(23)	O(24)	O(24^{iv})
O(22)	**1.60(2)**	2.57(1)	2.82(1)	2.82(1)
O(23)	104.0(7)	**1.65(1)**	2.85(1)	2.86(1)
O(24)	109.5(4)	109.2(4)	**1.84(1)**	3.11(1)
O(24^{iv})	109.5(4)	109.2(4)	115.0(4)	**1.84(1)**

P(1)	O(10)	O(12)	O(17)	O(24)
O(10)	**1.535(9)**	2.52(1)	2.41(1)	2.52(1)
O(12)	110.9(4)	**1.52(1)**	2.57(1)	2.49(1)
O(17)	103.1(5)	114.4(5)	**1.538(8)**	2.52(1)
O(24)	110.1(5)	108.8(5)	109.6(5)	**1.55(1)**

P(2)	O(3)	O(8)	O(25)	O(18^{v})
O(3)	**1.55(1)**	2.52(1)	2.49(1)	2.55(1)
O(8)	108.2(5)	**1.562(9)**	2.53(1)	2.41(1)
O(25)	109.8(6)	111.2(5)	**1.505(9)**	2.54(1)
O(18^{v})	111.7(5)	102.1(5)	113.7(5)	**1.535(8)**

P(3)	O(5)	O(9)	O(14)	O(26)
O(5)	**1.55(1)**	2.53(1)	2.40(1)	2.54(1)
O(9)	108.9(5)	**1.56(1)**	2.55(1)	2.48(1)
O(14)	102.2(5)	110.5(5)	**1.543(8)**	2.55(1)
O(26)	113.1(5)	108.0(5)	114.1(4)	**1.50(1)**

P(4)	O(13)	O(21)	O(16^{v})	O(4^{iii})
O(13)	**1.531(9)**	2.51(1)	2.52(1)	2.38(1)
O(21)	109.4(5)	**1.54(1)**	2.51(1)	2.50(1)
O(16^{v})	112.2(5)	109.6(5)	**1.49(1)**	2.47(1)
O(4^{iii})	102.2(5)	110.5(5)	112.8(5)	**1.53(9)**

Ba(1)—O(25)	2.69(1)	Ba(2)—O(5^{vi})	2.71(1)	Ba(3)—O(26)	2.66(1)
Ba(1)—O(25^{iv})	2.69(1)	Ba(2)—O(4^{iii})	2.74(1)	Ba(3)—O(26^{iv})	2.66(1)
Ba(1)—O(26)	2.73(1)	Ba(2)—O(10)	2.77(1)	Ba(3)—O(25)	2.70(1)
Ba(1)—O(26^{iv})	2.73(1)	Ba(2)—O(17)	2.81(1)	Ba(3)—O(25^{vii})	2.70(1)
Ba(1)—O(23)	2.75(1)	Ba(2)—O(18^{vi})	2.85(1)	Ba(3)—O(15^{viii})	2.72(1)
Ba(1)—O(19)	2.83(1)	Ba(2)—O(13)	2.92(1)	Ba(3)—O(15^{ix})	2.72(1)
Ba(1)—O(22)	2.90(1)	Ba(2)—O(14^{vi})	2.97(1)	Ba(3)—O(20^{x})	2.89(1)
Ba(1)—O(9)	3.13(1)	Ba(2)—O(2^{vi})	3.26(1)	Ba(3)—O(19)	3.02(1)
Ba(1)—O(9^{iv})	3.13(1)				

Symmetry codes: i 1+*x*, *y*, *z*; ii 1/2+*x*, 1/2—*y*, 1/2+*z*; iii *x*, *y*, 1+*z*; iv *x*, -*y*, *z*; v 1—*x*, *y*, *z*; vi -1/2+*x*, 1/2—*y*, 1/2+*z*; vii 1+*x*, *y*, 1+*z*; viii *x*, *y*, *z*—1; ix *x*,—*y*, 1+*z*; x 1+*x*, *y*, 1—*z*.

hedron, whereas the P(2) and P(3) tetrahedra share only three apices with one VO_6 octahedron and two VO_5 pyramids, the fourth free apex pointing toward the axis of the butterfly tunnels. The P—O distances ranging from 1.49 to 1.56 Å are close to those generally observed for monophosphate groups.

Each tetrahedron [V(5) and V(6)] exhibits two short V—O bonds (1.59–1.65 Å) and two longer ones (1.84–1.86 Å). The short V—O distances correspond to the free apices [O(19), O(20), O(22) and O(23)], whereas the longer ones correspond to V—O—P bonds. The mean <V—O> distance of 1.73 Å is close to that observed in vanadates as shown for instance in Li_3VO_4 [16] and $Ca_3(VO_4)_2$ [17] that exhibit average V—O bonds of 1.72 and 1.69 Å respectively.

The geometry of the VO_6 octahedra [V(3) and V(4)] is characteristic of the vanadyl species. Each octahedron exhibits one abnormally short V—O bond (1.561 and 1.597 Å) opposed to a very long apical bond (2.672–2.636 Å) and four intermediate equatorial V—O bonds (1.855–1.968 Å). The abnormally short V—O bond corresponds to the free apex [O(15) and O(11)] whereas the equatorial distances correspond to three V—O—P bonds and one V—O—V bond with a VO_5 pyramid. The abnormally long apical V—O distance characterizes oxygen atoms [O(1) and O(6)] shared with the VO_5 pyramid. This geometry leads us to describe the configuration of V(3) and V(4) as intermediate between a pyramid and an octahedron, rather than a pure octahedron. Therefore the V(3) and V(4) sites are either vanadium(IV) or vanadium(V). The bond valence calculations give 4.86 and 4.31 respectively for V(3) and V(4), indicating that vanadium(IV) lies preferentially on the V(4) sites.

The VO_5 pyramids [V(1) and V(2)] are rather distorted. Their apical V=O distances are very short (1.594–1.585 Å) and correspond to oxygen atoms [O(1) and O(6)] shared with the very long apical V—O bond of the VO_6 octahedron, so that these oxygens can be considered as almost free forming a vanadyl bond. The three equatorial distances are normal, ranging from 1.925 to 1.97 Å for V(1) and from 1.890 to 1.933 Å for V(2); they correspond to V—O—P bonds. The

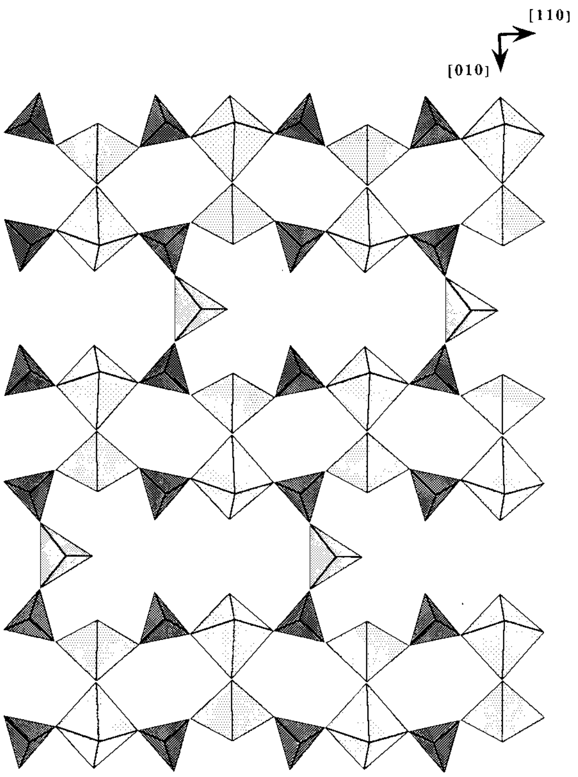

Fig. 5 Projection of a [$\bar{1}$10] layer

fourth equatorial distance is intermediate (1.717, 1.757 Å) and corresponds to the oxygen atoms [O(2), O(7)] which form another equatorial V—O bond with the VO_6 octahedron.

The barium cations, Ba(1) and Ba(3), which sit in the butterfly shaped tunnels (Fig. 1 and 3) exhibit a nine- and eight-fold coordination, respectively. Ba(1) exhibits a tricapped trigonal prismatic coordination with Ba—O distances ranging from 2.66 to 3.02 Å, whereas Ba(3) has a bicapped trigonal prismatic coordination with Ba—O distances ranging from 2.71 to 3.26 Å. The Ba(2) cation which is located in the six-sided tunnels within the $[V_4P_4O_{23}]_\infty$ layers (Fig. 1) has a distorted cubic coordination with Ba—O distances ranging from 2.71 to 3.26 Å.

References

1 J. Ziolkowski, E. Bordes and P. Courtine, *J. Catal.*, 1990, **122**, 126.
2 Y. Zhang-Lin, J. C. Vedrine and J. C. Volta, *J. Catal.*, 1994, **145**, 256.
3 J. Ziolkowski, E. Bordes and P. Courtine, *J. Mol. Catal.*, 1993, **84**, 307.
4 K. Bruckman, J. Haber and E. M. Servicka, *Faraday Discuss. Chem. Soc.*, 1989, **87**, 173.
5 P. M. Micchalakos, M. C. King, Jahan and H. H. Kung, *J. Catal.*, 1990, **140**, 226.
6 A. Leclaire, J. Chardon, A. Grandin, M. M. Borel and B. Raveau, *Eur. J. Solid State Chem.*, 1993, **30**, 461.
7 A. Leclaire, A. Grandin, J. Chardon, M. M. Borel and B. Raveau, *Eur. J. Solid State Chem.*, 1993, **30**, 343.
8 K. H. Lii, B. R. Chuch, H. Y. Kang and S. L. Wang, *J. Solid State Chem.*, 1992, **99**, 72.
9 A. Grandin, J. Chardon, M. M. Borel, A. Leclaire and B. Raveau, *J . Solid State Chem.*, 1992, **99**, 297.
10 A. Grandin, J. Chardon, M. M. Borel, A. Leclaire and B. Raveau, *Acta Crystallogr., Sect. C.*, 1992, **48**, 1913.
11 L. Benhamada, A. Grandin, M. M. Borel, A. Leclaire and B. Raveau, *Acta Crystallogr., Sect. C.*, 1991, **47**, 2437.
12 S. J. Hwu, R. I. Carroll and D. L. Serra, *J. Solid State Chem.*, 1994, **110**, 290.
13 K. Kasthuri Rangan and J. Gopalakrishnan, *J. Solid State Chem.*, 1994, **109**, 116.
14 H. Y. Kang and S. L. Wang, *Acta Crystallogr., Sect. C.*, 1992, **48**, 975.
15 S. Ledain, A. Leclaire, M. M. Borel, J. Provost and B. Raveau, *J. Solid State Chem.*, 1996, **125**, 147.
16 S. R. Hall, H. D. Flack and J. M. Steward, *XTAL3.2 Reference Manual*, Universities of Western Australia, Geneva and Maryland, 1992.
17 R. D. Shannon and C. Calvo, *J. Solid State Chem.*, 1973, **6**, 538.
18 R. Gopal and C. Calvo, *Z. Kristallogr.*, 1973, **137**, 67.

Paper 7/06529I; *Received* 8*th September*, 1997